

# Towards robust stability of aircraft electrical power systems

Sharmila Sumsurooah, Milijana Odavic, Serhiy Bozhko, and Dushan Boroyevic

**T**ransport accounts for nearly two thirds of the global crude oil consumption and about a quarter of carbon dioxide ( $CO_2$ ) emissions [1], [2]. The energy use and  $CO_2$  emissions in this sector are predicted to increase by 80% by 2050 [1]. The major contributors of greenhouse effects are expected to be light duty vehicles (43%), trucks (21%), aviation (20%) and shipping(8%) by 2050 [1]. Buses and rails are already sustainable modes of transport. In order to mitigate the impact of the emissions on climate change, the Intergovernmental Panel on Climate Change, which is the leading international body for assessment of climate change, recommends a reduction of at least 50% in global  $CO_2$  emissions by 2050 [1]. This target cannot be met unless there is a deep cut in  $CO_2$  emissions from the transportation sector. On the other hand, independently of climate policy actions, the projections are that fossil fuel reserves will become exhausted within the next 50 years. If a more sustainable future is to be achieved, the issues of greenhouse emissions and energy security are to be addressed at this very point in time. One of the long-term solutions may well lie in both the adoption of current best technologies and in the development of more advanced technologies, in all sectors of transportation [1]. A shift towards more efficient modes of transport, including the “more electric aircraft” (MEA), are not only needed but seem inevitable.

## MORE ELECTRIC AIRCRAFT

In conventional aircraft, power is generated by engines from fuel. The bulk of the power is used for propulsion; the remainder is transformed to hydraulic, pneumatic, mechanical and electrical power to supply different loads in the aircraft [4], [5]. Pneumatic power is used for the environmental control system (ECS) and wing anti-icing. Hydraulic energy is used to power flight controls and landing gear. Mechanical systems are driven by mechanical power through gearboxes. Electrical power is used for lighting, avionics and commercial loads. Moving towards the MEA involves increasing the electrical power generation and distribution capability of the aircraft to supply most of the aforementioned loads. This shift towards electricity rests on the development of power electronics (PE). It is the enabling technology that can contribute to high efficiency improvements in the aircraft, based on its distinctive features such as high power capability and controllability.

Power electronic technology is paving the way towards the more-electric engine and more-electric loads in the aircraft. The engines of the MEA will be started with inbuilt starter/generator instead of high pressure air [6]. The vanes to control airflow to the engine central core will be driven by PE converters. Power electronics will enable fuel pumps to run at their optimum speed in according with prevailing operating conditions [6]. This will significantly reduce wasted pumping energy. A large part of the aircraft loads, which

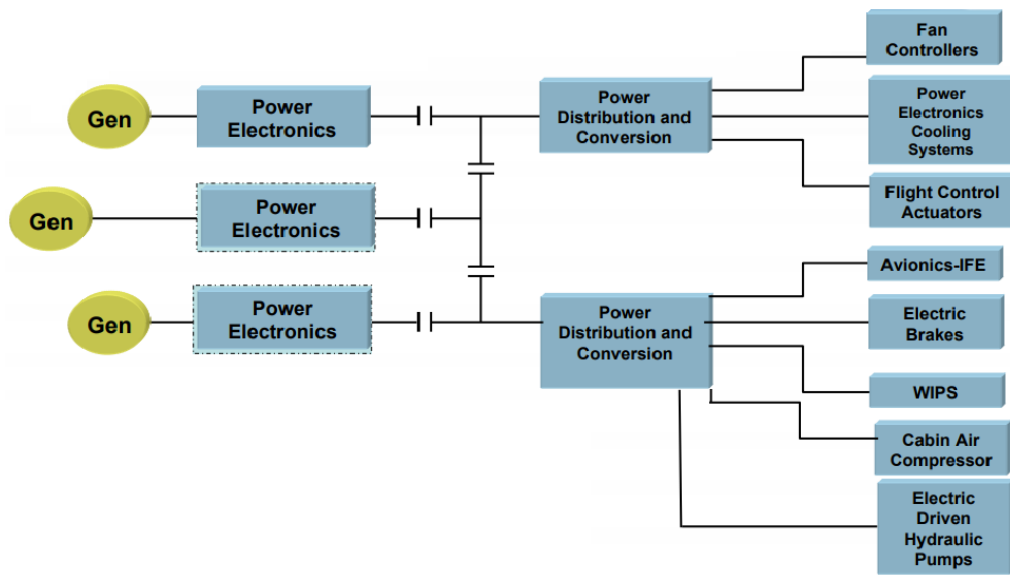


Fig. 1: Boeing 787 has a total of 1 MW of power electronic loads [3]

run on pneumatic or hydraulic energy, will be controlled by PE converters, leading to further increase in efficiency [6]. These include environmental control system and wing anti-icing. Pressurisation will be performed by electrically powered compressors. Most hydraulic and pneumatic actuators will be replaced by electromechanical actuators (EMA) [4]. Further, flight control systems and flight control actuation are expected to be PE-based. Of note is that many of these functions are already implemented on current aircraft such as the Boeing 787 Dreamliner [6]. The Boeing 787 has a total of 1 MW of power electronic loads as shown in Fig 1 [3].

#### SYSTEM STABILITY

Power electronic driven loads have numerous benefits as discussed earlier. However, one key drawback is that they are prone to instability. As the aircraft electrical network becomes larger and more complex, the multitude of PE-based loads can challenge the stability of the electrical power system (EPS) [7], [8]. This is owing to the fact that the loads interfaced through PE converters exhibit constant power load (CPL) behaviour, under fast controller actions [9], [10]. They are seen in the network as negative impedances [10]. It is the

negative impedance of the PE-based loads that may drive the system to instability. Two important components in the MEA architecture are the dc/dc converter and the dc/ac converter. The CPL behaviour of the loads interfaced with these two types of PE converters are presented herein for illustration.

The dc/dc converter is commonly used to supply certain avionics dc loads [6]. Fig. 2 depicts such a converter connected to a resistive load [6]. Power system applications for the dc/dc converter require the output voltage  $v_o$  to remain fairly constant despite perturbations in the input line voltage and step changes in load currents. This is achieved by having a compensator in the negative feedback loop of the converter, which automatically adjusts the duty cycle under various conditions of disturbances, so as to keep the output voltage  $v_o$  constant and close to the reference voltage  $v_{ref}$  [11]. Since the electrical load as well as the output voltage are constant in steady state condition, the power supplied to the load is constant. With the converter efficiency considered unvarying, the input power  $P_{in}$  drawn from the source is also constant.

Another key component of the aircraft EPS is the dc/ac converter. It is employed to drive loads such as flight control actuators [6]. Fig. 3 depicts such a system where the controller

regulates the speed  $w_r$  of a permanent magnet (PM) machine such that it follows the reference speed  $w_r^*$  [12]. Since the speed  $w_r$  as well as the torque  $T$  are constant at a given operating point, the power supplied to the load is constant. Considering that the losses of the motor and converter are constant, the input power  $P_{in}$  drawn from the source is also constant.

The aforementioned examples of the PE driven loads exhibit CPL behaviour. Under infinitely fast controller actions, they can mathematically be represented as a voltage controllable current source, as shown in Fig. 4. At any given operating point, the input voltage and input current to the converter system may be represented by dc values ( $V_{in}$ ,  $I_{in}$ ), as shown in Fig. 5. If the voltage increases by  $\delta v_{in}(t)$ , the input current has to decrease by  $\delta i_{in}(t)$  to keep the input power  $P_{in}$  constant [10]. Hence, while the instantaneous impedance  $V_{in}/I_{in}$  is positive, the incremental impedance given by  $\delta v_{in}(t)/\delta i_{in}(t)$  is negative as can be seen in Fig. 5.

The ideal CPL can be represented by a linearised model about a given operating point and is given by the negative impedance  $-R_{cpl}$  connected in parallel with a current source  $I_{cpl}$  as depicted by Fig. 6. At any arbitrary operating point, shown as  $E_{qo}$  in Fig. 5, the system currents and voltages may be represented by dc values with some superimposed small-ac components. In Fig. 6, the dc components of the supply voltage, supply current, input voltage and input current are clearly denoted as  $V_g$ ,  $I_g$ ,  $V_{in}$  and  $I_{in}$  respectively while their corresponding small-ac components are given by  $\hat{v}_g(t)$ ,  $\hat{i}_g(t)$ ,  $\hat{v}_{in}(t)$  and  $\hat{i}_{in}(t)$  respectively.  $R_{cpl}$  is given by  $V_{in}/I_{in}$  [13].

The negative impedance of the PE-based loads, as discussed earlier, under certain circumstances, may cause the system to oscillate and become unstable [14]. Stability assessment is thus crucial in the design of power electronic systems. It is to be emphasised that system stability has to be analysed both at the small and large signal level. Small-signal analysis investigates

the stability of an EPS when it is subject to small disturbances [12], [10], [15], [16]. The analysis is performed on a linearised system model about a certain operating point [12], [10], [15], [16]. In contrast, large signal stability analysis investigates the system's behaviour under large disturbances including sudden large changes in loads [17], [18], [19]. Although stability assessment of large signal disturbances is important, this work discusses small-signal stability analysis, which is an important concern in the reliable operation of the system.

As power electronics play a key role in developing more sustainable modes of transport, there is a dire need to address the issue of stability. Stringent assessment techniques are required to ensure the stability of electrical network for the MEA. The stability the permanent magnet machine drive ac/dc system and the dc/dc buck converter system, being important components of the MEA, will be discussed further in the work along with a representative EPS with an ideal CPL.

## STABILITY ROBUSTNESS

The stability of electrical power systems is generally assessed by using classical stability analysis techniques [20], [21]. These include the eigenvalue method, and impedance methods based on the Nyquist stability criterion. An EPS can be viewed as a cascade of its source and load components [15], [22], [23]. As illustrated in Fig. 4,  $Z_o$  and  $Z_i$  are the output and input impedances of the source and load subsystems respectively. The impedance ratio of  $Z_o$  to  $Z_i$ , is known as the minor loop gain  $T$ . According to the Nyquist stability criterion, for the system to be stable,  $1 + T$  must not have any roots in the right half plane [14], [15]. The more-than-necessary condition of Middlebrook criterion, which is an extension of the aforementioned formal requirement of the Nyquist stability criterion, requires that  $|Z_o| \ll |Z_i|$  for all frequencies, to ensure system stability [14] [24].

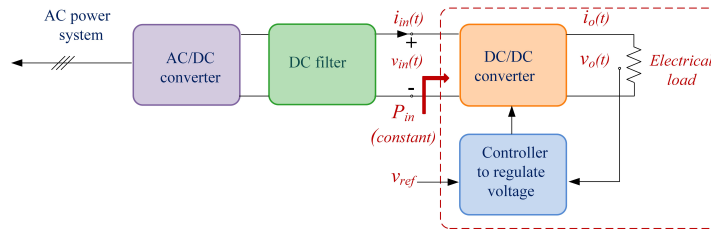


Fig. 2: A dc voltage regulator behaving as a CPL to the AC power supply

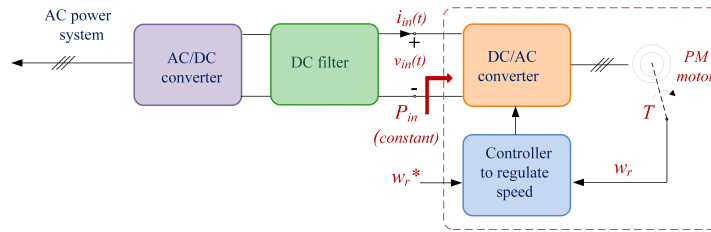


Fig. 3: An actuator system behaving as a CPL to the AC power supply

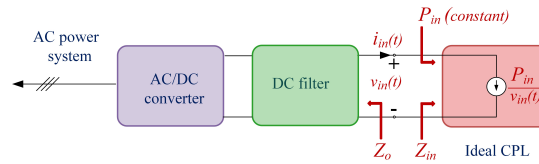


Fig. 4: An ideal CPL representing tightly controlled power conversion systems

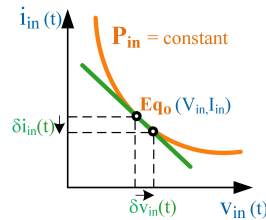


Fig. 5: Characteristic curve of an ideal CPL

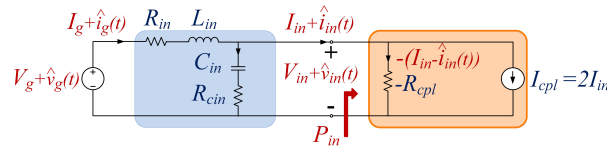


Fig. 6: Linear model of the system with ideal CPL

The classical methods treat the physical system as nominal model with fixed parameter values [20], [21]. The outcome of the stability assessment is therefore heavily dependent on the quality of the system model. The model may be refined to great detail by matching its response to that of the

physical system. Yet, in practice, excessive model refinement is unlikely to be viable or practical. Further, the exact values of system components may not be known accurately. For instance, system parasitics, often hard to quantify, can have a significant influence on the quality of the model. The power

supply and external filters, to be connected on site, may be unknown at the design stage. This may significantly alter the impedance of the power stage. In addition, electrical power systems may be exposed to large variations in their loads. Thus, it can be safely argued that, in practice, nominal system models are bound to contain uncertainties.

From another perspective, even though a nominal model is deemed to be accurate, it may not truly represent the actual system, which is generally subject to various operating conditions uncertainties. For instance, in aerospace applications power electronics based systems may be exposed to temperatures typically ranging from  $-40\text{ }^{\circ}\text{C}$  to  $125\text{ }^{\circ}\text{C}$  [25]. These large variations in temperature may have considerable effect on the properties of system components. Ageing is another factor which brings uncertainty to the system elements over time. Although an EPS is assessed as stable based on fixed parameters and conditions, it is questionable whether it continues to be stable in the face of all the aforementioned possible types of uncertainties.

Despite the fact that exact values of system components, system loads or operating conditions may not be known accurately, their range of variation can generally be estimated to good accuracy. For instance, the tolerance of most components can be obtained from data sheets. The variation of resistances can be computed from the range of change in operating temperatures. Uncertainty sets of power supply and filter impedances may be obtained based on possible make and type. Given that uncertainties seem to be inherent in EPS, it may be more natural to work around uncertain system models. In contrast with nominal models, uncertain models define both the nominal values and the possible range of variation of their parameters. The uncertain model is thus closer to the physical system. While classical methods are applied for stability analysis of nominal system models, a robust approach is needed for the stability assessment of uncertain system

models. The structural singular value (SSV)-based  $\mu$  approach is a robust stability method that incorporates all sources of uncertainties within the system [26], [27], [28], [29].

It can be argued that uncertainties can be incorporated when using classical methods. However, applying single input single output (SISO) methods to multi input multi output systems (MIMO) may not produce reliable results, as reported in a number of studies [30], [31].

The  $\mu$  approach is a deterministic method, that can provide a direct measure of stability robustness of a system with respect to its uncertain elements. The robust stability measure  $\mu$  should be less than 1 for a system to be robustly stable [32], [29]. The  $\mu$  method is founded on the aforementioned concept of the uncertain system model. Hence, by working directly on an uncertain model,  $\mu$  analysis eliminates the burden from a user of performing exhaustive parameter iterations and system linearisation [33], [34]. The  $\mu$  approach has proven to produce reliable results in robust stability analysis of power systems subject to multiple simultaneous uncertainties [26], [31], [32], [29], [35].

Following the above discussion, it is evident that there is a need to ensure that an EPS is not only stable but robustly stable, i.e. it must remain stable in the face of all system uncertainties. This is especially important for safety-critical applications.

#### CONSTANT POWER LOAD

Robust stability domains can be viewed as subsets of the much wider stability domains in the multi-dimensional parametric space. In order to illustrate the concept of stability robustness, the  $\mu$  tool is employed to identify the robust stability domains of the representative EPS connected to an ideal CPL, as shown in Fig. 6, when it is subject to single and multiple parametric uncertainties. In this section, the  $\mu$  results, which are generated in the frequency domain, have

been translated to the more perceivable uncertain parameters domain to better illustrate the concept of robust stability domains.

The first study in this section evaluates the robust stability of the analysed system when it is exposed to a single parametric uncertainty. The input power  $P_{in}$  is allowed to vary within  $10.4 \text{ W} \pm 33\%$  of its nominal value. The values of the line resistance  $R_{in}$ , input filter capacitance  $C_{in}$  and input filter inductance  $L_{in}$  are kept fixed at their nominal values of  $160 \text{ m}\Omega$ ,  $95 \text{ }\mu\text{F}$  and  $511.8 \text{ }\mu\text{H}$  respectively.  $\mu$  analysis of the uncertain system yields the  $\mu$  chart in Fig. 7, from which it can be seen that the peak values of the lower bound  $\underline{\mu}$  and the upper bound  $\bar{\mu}$  are equal to 3.02 [13]. The critical destabilising frequency is 720 Hz which corresponds to the resonant frequency of the inductor-capacitor (LC) filter. From the  $\mu$  value, the critical destabilising value of the input power can be computed as 11.53 W [13].

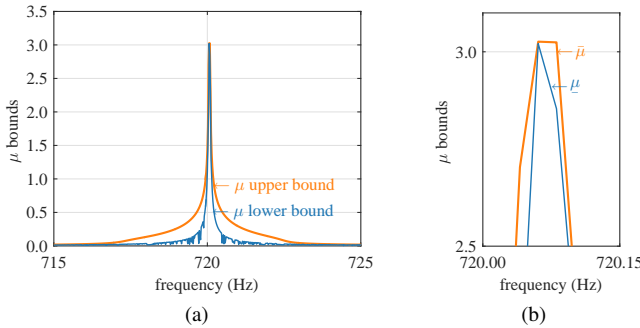


Fig. 7: Single uncertain parameter system (a)  $\mu$  chart to predict critical  $P_{in}$  (b) zoomed area near peak of  $\mu$  chart

Based on the technique of linear fractional transformation, the normalised uncertain parameters  $\delta_{P_{in}}$  may be extracted from the state space system model and grouped in a diagonal matrix  $\Delta$  in feedback form [13]. In this case study, uncertainty matrix  $\Delta$  has the size of  $3 \times 3$ , as the uncertain parameter  $P_{in}$  appears 3 times in the state space system model.  $\mu$  analysis identifies the smallest disturbance matrix that can destabilise the system. The normalised uncertain parameter  $\delta_{P_{in}}$  in the critical uncertainty matrix  $\Delta$  is equal to +0.331.

For the single parametric uncertainty, the  $\mu$  tool has identified the largest line segment of coordinate size  $1/\mu = 0.331$  centred about the nominal point, within which the system is guaranteed robustly stable, as illustrated in Fig. 8. The given line segment corresponds to the robust uncertainty sets of  $[9.3 \text{ W}, 11.5 \text{ W}]$  for the input power. Provided that the system under investigation operates with an input power which lies within the aforementioned robust stability margin, the system is ensured to be robustly stable.

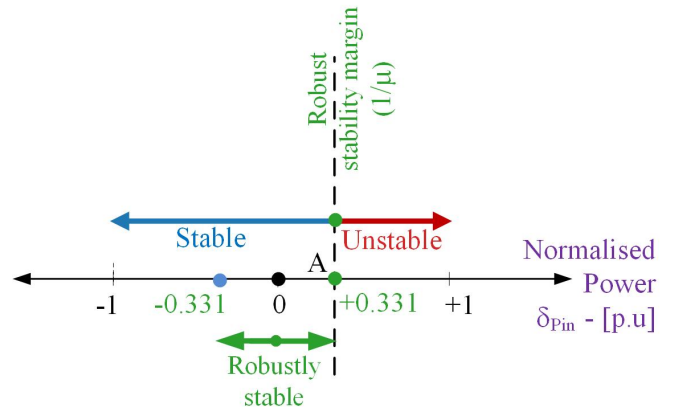


Fig. 8: Single uncertain parameter system - Largest linear segment of coordinate size  $(1/\mu = 0.331)$  centred about nominal point, connecting point A at the boundary stability, within which system is robustly stable

The second case considers that the system under study is exposed to an additional parametric uncertainty, namely to the input capacitance uncertainty  $C_{in}$  which is allowed to vary within  $95 \text{ }\mu\text{F} \pm 10\%$ . For this case study, the resulting  $\mu$  is equal to 4.03, and the robust stability margin is  $|\delta_{P_{in}}| = |\delta_{C_{in}}| = 1/\mu = 0.248$ .

In parametric space, for a system subject to two parametric uncertainties, the  $\mu$  tool identifies the largest square of coordinate size  $1/\mu$ , which is equal to 0.248 for this case study, centred about the nominal point within which the system can be guaranteed to be robustly stable, as illustrated in Fig. 9. It can be shown that the ‘square’ corresponds to the robust uncertainty sets  $[9.5 \text{ W}, 11.3 \text{ W}]$  and  $[92.6 \text{ }\mu\text{F}, 97.4 \text{ }\mu\text{F}]$  for the input power and capacitance respectively. It implies that if

the analysed system operates within the given boundary, the system is guaranteed robustly stable.

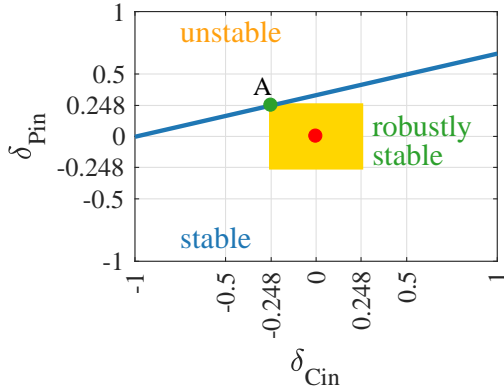


Fig. 9: Two uncertain parameters system - Largest square of coordinate size ( $1/\mu = 0.248$ ) centred about the nominal point, connecting point A which lies on the stability line, within which system is robustly stable

A last case is presented in this section whereby in addition to uncertainties in the input power and the input filter capacitance, the input filter inductance  $L_{in}$  is also allowed to vary within  $\pm 10\%$  of its nominal value of  $511.8 \text{ mH}$ . For this three uncertain parameters system, the peak value of  $\mu$  is  $4.974$ , and the corresponding robust stability margin  $1/\mu$  is  $0.201$ . When considering a system subject to three parametric uncertainties,  $\mu$  analysis identifies the largest cube within which system robust stability is guaranteed, which in this case study is of coordinate size  $|\delta_{Pin}| = |\delta_{Cin}| = |\delta_{Lin}| = 1/\mu = 0.201$  about the nominal point. It can be shown that the hypercube corresponds to the input power, capacitance and inductance lying within the robust uncertainty sets of  $[9.7 \text{ W}, 11.1 \text{ W}]$ ,  $[93.1 \mu\text{F}, 97.0 \mu\text{F}]$  and  $[501.5 \text{ mH}, 522.1 \text{ mH}]$  respectively.

By extrapolating on the ideas presented in this section, for a system subject to  $N$  parametric uncertainties,  $\mu$  analysis provides the largest hypercube of dimension  $N$  centred about the nominal point and of coordinate size  $1/\mu$ , within which system robust stability can be guaranteed [13], [35].

This section has shown, through application and illustrations, the robust stability domains as subsets of the wider

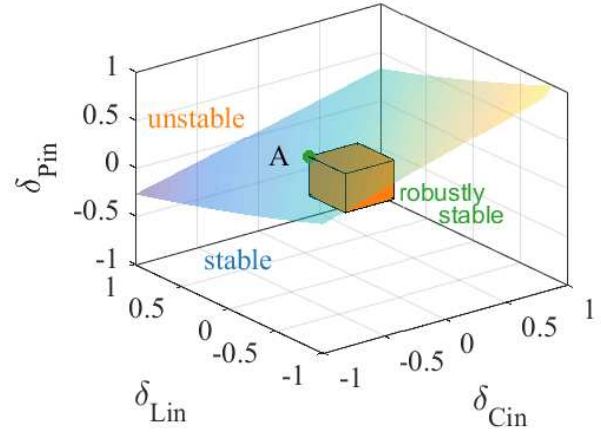


Fig. 10: Three parameters system - Largest cube of coordinate size ( $1/\mu = 0.201$ ) centred about nominal point, connecting point A which lies on the stability plane, within which system is robustly stable

stability domains in the multi-dimensional parametric space. The concept presented in this section has many practical implications. It offers the design engineer a parametric space within which to manoeuvre and choose optimum parameters while ensuring stability robustness. The  $\mu$ -based robust stability domains can be extended to more complex studies. The stability robustness of two dominant sub distribution systems in the MEA architecture, namely the permanent magnet machine drive (PMMD) system and the buck converter system, are assessed based on the  $\mu$  method in the ensuing sections.

#### PERMANENT MAGNET MACHINE DRIVE SYSTEM

The stability of a PMMD system, generally employed for an actuation system in an aircraft EPS, was studied in the laboratory [36], [37]. The circuit representation of the analysed system is depicted by Fig. 11 [36], [37]. An ideal 3-phase balanced voltage source was used in experiment to represent the engine generator with the generator control unit denoted as  $G$  and  $GCU$  respectively in Fig. 11. The transmission line or ac bus from the power supply to the rectifier was modelled by a resistor-inductor circuit. A six-pulse uncontrolled rectifier was employed as a typical multiphase autotransformer-rectifier

(ATRU) unit of a real on-board system. It provided dc power to the surface mounted PM machine based electromechanical actuator (EMA) through an LC filter. The EMA was a standard vector-controlled PM motor drive [36], [37]. The detailed modelling and robust stability analysis of the system are presented in [33].

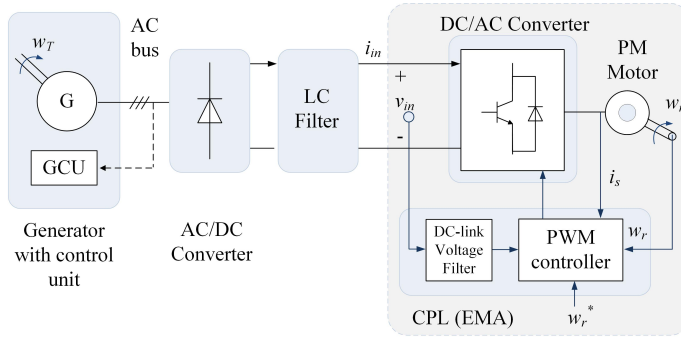


Fig. 11: Permanent magnet machine based electromechanical actuator (EMA)

The aim of the study was to identify whether the system remains stable when the applied torque is allowed to vary within the uncertainty set [2 Nm, 38 Nm], (i.e  $20 \pm 18$  Nm), where 20 Nm is the mean value of the torque on the given uncertainty set [33]. The system in Fig. 11 was analytically modelled to account for uncertainty in torque and system non-linearities [33].  $\mu$  analysis was employed to predict boundary stability. From  $\mu$  analysis of the system model, the measure of robust stability  $\mu$  was found to be 2.31. The robust stability margin, calculated as  $1/\mu = 0.42$ , corresponds to a critical destabilising torque of 27.6 Nm. Laboratory tests showed that the PMMD system becomes unstable when the torque is increased to 26.7 Nm, which is in close agreement with the  $\mu$  prediction of 27.6 Nm.

The analysis showed that the EMA system under study is not robustly stable as indicated by  $\mu$  exceeding 1, i.e. it becomes unstable if operated within the defined uncertainty set (i.e. within  $20 \pm 18$  Nm). The robust stability margin of 0.42 represents the value by which the maximum range of uncertainty in torque must be scaled to ensure stability

robustness, as depicted in Fig. 12. This requires that the operation of the EMA system be limited within  $20 \pm 7.6$  Nm. Therefore from the above discussion, it can be concluded that  $\mu$  provides a direct measure of stability robustness of an EPS, as it determines by how much uncertain parameters can be changed without causing a system to become unstable.

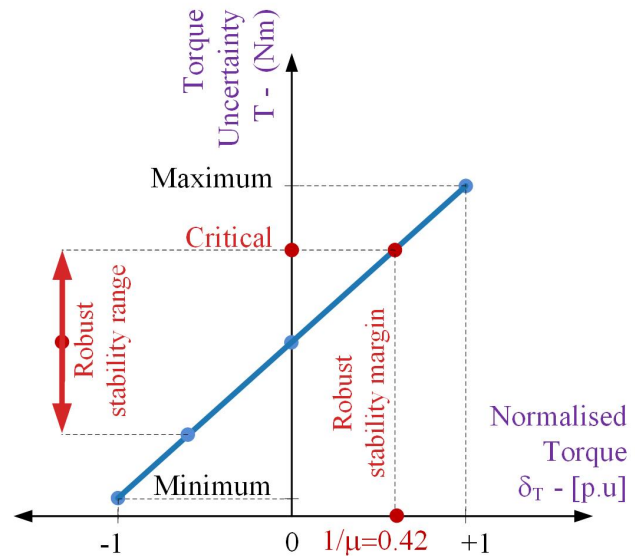


Fig. 12: Robust stability margin of the EMA system under uncertainty in torque

#### BUCK CONVERTER SYSTEM

In practice, actual systems are continually subject to perturbations. These include but are not limited to variations in load, line resistance and operating temperature. Further, the nominal system model generally contains parametric model uncertainties. While uncertainties are a known occurrence in actual systems, the question is whether it is acceptable or even safe to neglect them during the design process. In order to answer this question, a series of studies was performed on the widely employed dc/dc buck converter system to gauge the impact of the aforementioned uncertainties on stability robustness of a system. The block diagram of the system under study is shown in Fig. 2. The experimental buck converter system that was used in the study consisted of a U3825



PWM controller, a Type III analogue compensator and an LC input filter. The buck converter, supplied from an ideal voltage source through a line cable was set to regulate the output voltage to a resistive load. The detailed modelling and analysis of the system is presented in [38].

Seven case studies were performed using  $\mu$  analysis tool, as given in Table I. The buck converter system has a conversion rate equal to its duty cycle, which has non-linear dependence on the output resistive load. The non-linearities in the duty cycle has to be accounted for in the modelling of the analysed system [38]. Further, the duty cycle, which has been obtained as an irrational term in the system model, has to be approximated by polynomial expansion to suit  $\mu$  analysis. Case studies 1.1-1.2 and 2.1-2.2 employed the first and zeroth order of approximation for the duty cycle respectively. Since case studies 3.1-3.3 investigated the impact of model uncertainties on stability robustness, they treated the duty cycle as an uncertain parameter about its nominal value. It is also added that the case studies 1.1, 1.2, 2.1, 2.2 employed accurately measured nominal values for the system parameters, while case studies 3.1-3.3 were based on available rough estimates of the nominal values of the system parameters.

Case study 1.1 investigated the robust stability of the buck converter system when it is exposed to a large variation in its resistive load, i.e.  $2.5 \Omega \pm 50\%$ .  $\mu$  analysis determined that the analysed system becomes unstable when the output power is increased to  $16 W$ , based on a robust stability margin  $1/\mu$  of  $0.696$ , as shown in Table I. Of note is that the robust stability margin  $1/\mu$  of unity would mean that the system is guaranteed stable on the entire uncertainty set and for the output power up to  $20.8 W$ . The  $\mu$  predicted critical output power of  $16 W$  was verified in experiment. In laboratory, the electronic resistive load was decreased in small steps from a peak value of  $2 \Omega$ . At time  $0.453 s$ , when the resistive load was decreased to  $1.63 \Omega$  (i.e.  $16.0 W$ ), the system reached boundary stability,

as shown by the sustained oscillations in input voltage  $V_{in}$ , output voltage  $V_o$  and output current  $I_o$  in Fig. 13.

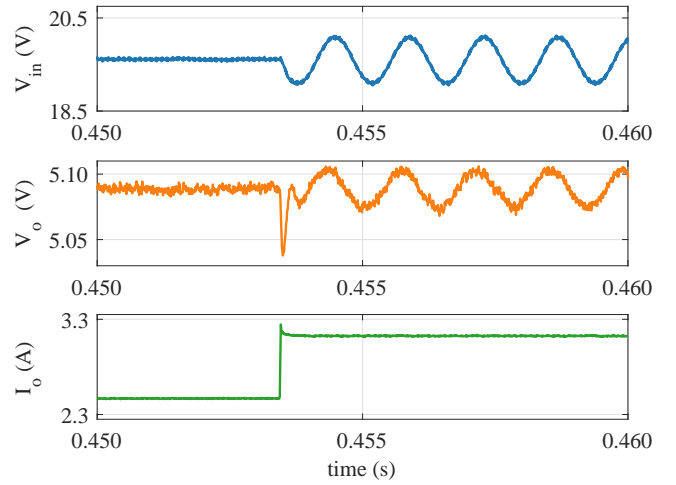


Fig. 13: Case 1.1 - Experimental results for the system with load uncertainty - system is at boundary of stability with  $R = 1.63 \Omega$  from  $t = 0.453 s$  to  $0.460 s$

The line resistance is not known accurately at design stage but is dependent on the final assembly of the system components. Case study 1.2 investigates the effect of the line resistance on robust stability margin, when both the load and the line resistance are uncertain. The line resistance is assumed to vary within  $\pm 50\%$  of its nominal value of  $0.3 \Omega$  while the variation in the resistive load is as described in case study 1.1. From  $\mu$  analysis, it has been found that if both the uncertain load and line resistance are kept within  $80.3\%$  of their respective nominal values, the system under study can be ensured to be stable for an output power of up to  $17.3 W$ . For the case 1.2, the robust stability margin increases as the line resistance  $R_{in}$ , set in the range of  $[150 m\Omega, 450 m\Omega]$ , provides more damping to the resonant LC input filter with respect to case 1.1, when  $R_{in}$  is set at a constant value of  $160 m\Omega$ . Therefore, for case 1.2,  $\mu$  analysis finds new uncertainty sets of  $[1.5 \Omega, 3.5 \Omega]$  and  $[180 m\Omega, 420 m\Omega]$  for the resistive load and line resistance respectively, and the system is robustly stable for  $R > 1.5 \Omega$  and  $R_{in} > 180 m\Omega$  and for an output power of up to  $17.3 W$ .

Temperature is one of the main factors that can introduce uncertainties in multiple system parameters. In case study 2.2, the buck converter system is considered to be working in an environment where temperature may vary between  $-40^{\circ}C$  and  $80^{\circ}C$  with a reference value of  $20^{\circ}C$ . The temperature variation influences the values of the resistive components of the buck converter such as the equivalent series resistance of the capacitors and inductors of the input and output filters, the line resistance and the switch on resistance of the MOSFET. The load is assumed to vary as in case 1.1. Case study 2.2 was then repeated with the same condition as case 2.1 but with temperature being fixed at its nominal value. Further to  $\mu$  analysis, the robust stability margin of the buck converter has been found to be 50.5% when uncertainties in temperature are included as shown in case study 2.1, as compared to 74.5% when uncertainties in temperature are not included in case study 2.2. The important difference in robust stability margin in these two case studies emphasises the necessity of incorporating operating temperature uncertainty for more reliable stability analysis of a system.

In practice, it is neither viable nor time-efficient to create highly refined system models to represent actual systems. Hence, approximate system models, with a good trade-off between accuracy and simplicity, are often used for design. The nominal values of their system components are generally based on known data such as nameplate information. Case studies 3.1-3.3 aim to demonstrate how model uncertainties, which may be known to different level of accuracy, can be incorporated in robust stability analysis without compromising the reliability of the results. In addition, it examines the effect of model uncertainties on robust stability margin. In case study 3.1,  $\mu$  analysis has predicted the critical output power of the considered buck converter to be 15.0 W with a robust stability margin of 61.4%, when model uncertainties are neglected and the model is assumed to be completely accurate. On the other

hand, the critical output power has been determined as 11.6 W in case study 3.2, when uncertainties are included, while its value increased to 12.2 W, when the given uncertainties are defined within a relatively narrower range in case study 3.3. With model uncertainties incorporated in the analysis, the robust stability margin is 0.210 and 0.288 for cases 3.2 and 3.3 respectively. Although, the results for cases 3.2 and 3.3 seem to be conservative in comparison to case 3.1, they are more reliable. This is because the analyses take into account uncertainties of the system model, and therefore include worst case scenarios.

The findings in these studies confirm that uncertainties have a significant impact on the stability robustness, and must be duly incorporated during design process, particularly for safety-critical applications

TABLE I: Buck converter - Robust stability studies results

Case study	Uncertain parameters	Robust stability margin $1/\mu$	Critical load power (W)
1.1	Load (with fixed line resistance)	0.696	16.0 W
1.2	Load and line resistance	0.803	17.3 W
2.1	Load and temperature	0.505	13.9 W
2.2	Load (with fixed temperature)	0.745	16.6 W
3.1	Load (with no model uncertainty)	0.614	15.0 W
3.2	Load and model uncertainties (wide range)	0.210	11.6 W
3.3	Load and model uncertainties (narrow range)	0.288	12.2 W

## CONCLUSION

Power electronics is the enabling technology that is paving the way towards more sustainable aviation. There is a pressing need for design engineers to address the issues such as power system stability that could slow down the transition towards the MEA. In doing so, design engineers may need to think beyond classical techniques and adopt novel analysis tools that can provide more effective solutions to the current issues associated in the development of the future electric aircraft. This paper has demonstrated the  $\mu$  based structural singular value as one possible technique to analyse and ensure stability robustness of the electrical network of the MEA.

## ACKNOWLEDGMENT

The authors gratefully acknowledge the support for the work from the EU as part of the Clean Sky project, part of EU FP7 program.

## REFERENCES

- [1] I. E. Agency, *Transport Energy and CO<sub>2</sub>: Moving Towards Sustainability*. OECD Publishing, 2009.
- [2] I. P. on Climate Change, *Climate change 2014: mitigation of climate change*, vol. 3. Cambridge University Press, 2015.
- [3] K. J. Karimi, "Future aircraft power systems-integration challenges," *The Boeing Company*, 2007.
- [4] P. Wheeler and S. Bozhko, "The more electric aircraft: Technology and challenges," *IEEE Electrification Magazine*, vol. 2, pp. 6–12, Dec 2014.
- [5] A. Boglietti, A. Cavagnino, A. Tenconi, S. Vaschetto, and P. di Torino, "The safety critical electric machines and drives in the more electric aircraft: A survey," in *2009 35th Annual Conference of IEEE Industrial Electronics*, pp. 2587–2594, Nov 2009.
- [6] I. Moir and A. Seabridge, *Aircraft systems: mechanical, electrical and avionics subsystems integration*, vol. 52. John Wiley & Sons, 2011.
- [7] K. N. Areerak, S. V. Bozhko, G. M. Asher, L. D. Lillo, and D. W. P. Thomas, "Stability study for a hybrid ac-dc more-electric aircraft power system," *IEEE Transactions on Aerospace and Electronic Systems*, vol. 48, pp. 329–347, Jan 2012.
- [8] F. Barruel, A. Caisley, N. Retiere, and J. L. Schanen, "Stability approach for vehicles dc power network: Application to aircraft on-board system," in *2005 IEEE 36th Power Electronics Specialists Conference*, pp. 1163–1169, June 2005.
- [9] K. N. Areerak, S. V. Bozhko, G. M. Asher, and D. W. P. Thomas, "Stability analysis and modelling of ac-dc system with mixed load using dq-transformation method," in *2008 IEEE International Symposium on Industrial Electronics*, pp. 19–24, June 2008.
- [10] A. B. Jusoh, "The instability effect of constant power loads," in *Power and Energy Conference, 2004. PECon 2004. Proceedings. National*, pp. 175–179, IEEE, 2004.
- [11] R. W. Erickson and D. Maksimovic, *Fundamentals of power electronics*. Springer Science & Business Media, 2001.
- [12] K. Areerak, *Modelling and stability analysis of aircraft power systems*. PhD thesis, University of Nottingham, 2009.
- [13] S. Sumsurooah, M. Odavic, and S. Bozhko, " $\mu$  approach to robust stability domains in the space of parametric uncertainties for a power system with ideal cpl," *IEEE Transactions on Power Electronics*, vol. PP, no. 99, pp. 1–1, 2017.
- [14] R. D. Middlebrook, "Input filter considerations in design and application of switching regulators," *IAS Record, 1976*, 1976.
- [15] A. Riccobono and E. Santi, "Comprehensive review of stability criteria for DC power distribution systems," *Industry Applications, IEEE Transactions on*, vol. 50, no. 5, pp. 3525–3535, 2014.
- [16] A. Emadi, A. Khaligh, C. H. Rivetta, and G. A. Williamson, "Constant power loads and negative impedance instability in automotive systems: definition, modeling, stability, and control of power electronic converters and motor drives," *IEEE Transactions on Vehicular Technology*, vol. 55, pp. 1112–1125, July 2006.
- [17] Y. Che, X. Liu, and Z. Yang, "Large signal stability analysis of aircraft electric power system based on averaged-value model," in *2015 6th International Conference on Power Electronics Systems and Applications (PESA)*, pp. 1–5, Dec 2015.
- [18] A. Griffo and J. Wang, "Large signal stability analysis of 'more electric' aircraft power systems with constant power loads," *IEEE Transactions on Aerospace and Electronic Systems*, vol. 48, no. 1, pp. 477–489, 2012.
- [19] S. Rosado, R. Burgos, F. Wang, and D. Boroyevich, "Large-signal stability analysis in power systems with a synchronous generator connected to a large motor drive," in *2007 IEEE Electric Ship Technologies Symposium*, pp. 42–47, May 2007.
- [20] G. F. Franklin, J. D. Powell, A. Emami-Naeini, and J. D. Powell, *Feedback control of dynamic systems*, vol. 2. Addison-Wesley Reading, 1994.
- [21] R. C. Dorf and R. H. Bishop, "Modern control systems," 1998.
- [22] A. M. Rahimi and A. Emadi, "An analytical investigation of dc/dc power electronic converters with constant power loads in vehicular power systems," *Vehicular Technology, IEEE Transactions on*, vol. 58, no. 6, pp. 2689–2702, 2009.
- [23] S. Sudhoff and O. Wasynczuk, "Analysis and average-value modeling of line-commutated converter-synchronous machine systems," *Energy Conversion, IEEE Transactions on*, vol. 8, no. 1, pp. 92–99, 1993.
- [24] C. M. Wildrick, F. C. Lee, B. H. Cho, and B. Choi, "A method of defining the load impedance specification for a stable distributed power system," *IEEE Transactions on Power Electronics*, vol. 10, no. 3, pp. 280–285, 1995.
- [25] W. E. Sollecito and D. A. Swann, "Computer evaluation of high-temperature aircraft a-c electrical system designs," *Transactions of the American Institute of Electrical Engineers, Part II: Applications and Industry*, vol. 78, pp. 434–444, Jan 1960.
- [26] J. Doyle, "Analysis of feedback systems with structured uncertainties," in *IEE Proceedings D (Control Theory and Applications)*, vol. 129, pp. 242–250, IET, 1982.
- [27] J. C. Doyle, B. A. Francis, and A. Tannenbaum, *Feedback control theory*, vol. 1. Macmillan Publishing Company New York, 1992.
- [28] M. Green and D. J. Limebeer, *Linear robust control*. Courier Corporation, 2012.

- [29] S. Skogestad and I. Postlethwaite, *Multivariable Feedback Control: Analysis and Design*. Multivariable Feedback Control: Analysis and Design, Wiley, 2005.
- [30] M. Kuhn, Y. Ji, and D. Schrder, "Stability studies of critical DC power system component for More Electric Aircraft using mu sensitivity," in *Control & Automation, 2007. MED'07. Mediterranean Conference on*, pp. 1–6, IEEE, 2007.
- [31] P. M. Young, M. P. Newlin, and J. C. Doyle, " $\mu$  analysis with real parametric uncertainty," in *Decision and Control, 1991., Proceedings of the 30th IEEE Conference on*, pp. 1251–1256, IEEE, 1991.
- [32] K. Zhou, J. Doyle, and K. Glover, *Robust and Optimal Control*. Feher/Prentice Hall Digital and, Prentice Hall, 1996.
- [33] S. Sumsurooah, M. Odavic, and S. Bozhko, "A modeling methodology for robust stability analysis of nonlinear electrical power systems under parameter uncertainties," *IEEE Transactions on Industry Applications*, vol. 52, pp. 4416–4425, Sept 2016.
- [34] S. D. Sudhoff, S. F. Glover, P. T. Lamm, D. H. Schmucker, and D. Delisle, "Admittance space stability analysis of power electronic systems," *Aerospace and Electronic Systems, IEEE Transactions on*, vol. 36, no. 3, pp. 965–973, 2000.
- [35] G. Ferreres, *A practical approach to robustness analysis with aeronautical applications*. Springer Science & Business Media, 1999.
- [36] K. N. Areerak, T. Wu, S. V. Bozhko, G. M. Asher, and D. W. P. Thomas, "Aircraft power system stability study including effect of voltage control and actuators dynamic," *IEEE Transactions on Aerospace and Electronic Systems*, vol. 47, pp. 2574–2589, OCTOBER 2011.
- [37] K.-N. Areerak, S. Bozhko, L. de Lillo, G. Asher, D. Thomas, A. Watson, and T. Wu, "The stability analysis of ac-dc systems including actuator dynamics for aircraft power systems," in *Power Electronics and Applications, 2009. EPE '09. 13th European Conference on*, pp. 1–10, Sept 2009.
- [38] S. Sumsurooah, M. Odavic, S. Bozhko, and D. Boroyevich, "Stability and robustness analysis of a dc/dc power conversion system under operating conditions uncertainties," in *Industrial Electronics Society, IECON 2015 - 41st Annual Conference of the IEEE*, pp. 003110–003115, Nov 2015.